Int. Journ. of Laser Science, Vol. 1, pp. 265–277
Reprints available directly from the publisher.
Photocopying permitted by license only.

Multi-response Optimization of CO_2 Laser Welding of Rene 80 Using Response Surface Methodology (RSM) and the Desirability Approach

M. MORADI[1,2,*] AND M.M. FALLAH[3]

[1]*Malayer University, Engineering Faculty, Mechanical Engineering Department, Malayer, Iran*
[2]*Laser Materials Processing Research Center, Malayer University, Malayer, Iran*
[3]*Shahid Rajaee Teacher Training University, Mechanical Engineering Department, Tehran, Iran*

Recently several efforts have been made for optimizing the laser welding process of superalloys due to their wide applications in the industry. In order to achieve the appropriate properties of weldments, the input parameters of the laser welding process should be studied and optimized. The present study was aimed at the statistical optimization of CO_2 laser butt joint welding of Ni-based super alloy Rene 80. So, the input parameters laser power, welding speed, laser beam focal point position and inert gas pressure have been optimized for achieving proper weld geometry comprised of welding surface width, welding pool area, welding width of heat affected zone (HAZ), weld undercut and drop of welding process. For modelling and optimizing of process parameters, the response surface methodology (RSM) benefiting from the desirability approach was utilized. Verification experiments were carried out in order to analyse the optimization results and the welding geometry, mechanical properties of tensile strength and microhardness of samples were studied.

Keywords: CO_2 laser, Ni-based super alloy, Rene 80, laser welding, geometrical dimensions, optimization, response surface methodology (RSM), desirability approach

1 INTRODUCTION

Among welding methods, laser beam is successfully used for welding metals and different alloys [1]. Nature of laser beam enables focusing in a very small

*Corresponding author: E-mail: moradi@malayeru.ac.ir

spot diameter and accessing to high power density. According to this, the laser welding will be regarded as keyhole mode fusion welding technique [2]. Suitable penetration, thin heat affected zone (HAZ), lower distortion, ability of welding without filler material, lower residual stresses and strains, flat surface of weld pool, are among advantages of laser welding that discriminates this method from other welding processes [3]. During last decades, the use of design of experiments (DOE) has significantly increased in different fields, such as physics, engineering and chemistry in order to modelling and optimization. Response surface methodology (RSM) is one of the proper statistical and mathematical optimization techniques used widely in describing the performance of the welding processes and finding the optimum settings of the parameters to achieve responses of interest [4] and is used for modelling and optimization of several laser based processes [5-7]

There are several research reports in the literature about modelling welding processes. Wang and Rasmussen [8] investigated and optimized the inertia welding process of low carbon steels using RSM. Benyounis *et al.* [9] applied response surface method to identify the optimal welding conditions in order to increase the productivity and minimize the total operating cost. Moradi and Ghoreishi [10] have developed mathematical models to study the effect of the laser welding parameters of Ni-based super alloy Rene 80 on weld bead profile using the RSM method. Anawa and Olabi [11] have optimized tensile strength of CO_2 laser welding by using a matrix design of the Taguchi method. The variable laser parameters in their study were: laser power, welding speed and focal point position. Comparison between numerical algorithm and DOE methods of optimization was performed by Olabi *et al.* [12] in order to gain minimum residual stress during laser butt joint welding. Torabi and Kolahan [13] applied RSM for statistical modelling between Nd:YAG laser welding process and product mechanical strength. They optimized the process using RSM and simulated annealing methods. Laser frequency and peak power are the more significant parameters that effect the ultimate tensile strength (UTS) of weldments. Kumara *et al.* [14] studied the fiber laser beam welding of Ti64 alloy and investigated the effect of process parameters on samples geometry and mechanical properties. They also optimized the process using RSM and confirmed that welding speed and power have highest impact on proper welding geometry. Pakmanesh *et al.* [15] optimized the Nd:YAG laser welding process of steel 326L for reducing the weld defects including underfill and undercut utilizing RSM and presented that power and frequency have more effect on weld defects. Khan *et al.* [16] presented an experimental work on CW Nd:YAG laser welding process optimization aiming the mechanical properties and geometrical dimensions of the samples using RSM. Laser power and welding speed are the most significant factors affect the weld quality. Pakniat *et al.* [17] compared weld penetration and hot cracking tendency in Nd:YAG laser process of Hastelloy X alloy in pulsed and continuous wave (CW) operation. The pulsed lase is more prone

to hot cracks relative to continuous one and increasing the laser pulse frequency would decrease the hot cracking tendency in pulsed laser welding. Also reduction in cooling rate could prevent the hot cracks in process of Hastelloy X.

In this study the optimization of the laser welding parameters were carried out in order to access minimum geometrical dimensions of weld-bead profile according to achieved mathematical models by authors' previous works [10]. In order to validate the results of optimization, some welding experiments were carried out at optimum settings; moreover, tensile strength and microhardness of welding in optimized settings were studied.

2 OPTIMIZATION METHODOLOGY

2.1 Response surface methodology (RSM)

RSM is one of the DOE and optimizing techniques and is widely used in describing different processes and suggestion of optimum answers [9, 10, 18, 19]. The RSM is a set of statistical and mathematical edicts which are used for modelling and predicting results, affected by input parameters. The RSM clarifies relations between answers and input under control parameters [4].

When all independent variable parameters during experiment are measurable and controllable, the response surface, Y, will be represented by [20]

$$Y = f\left(X_1, X_2, X_3, ..., X_k\right) \tag{1}$$

where k is number of independent variables. It is necessary to find a logical function in order to attribute the response to the independent variables; thus, a second order polynomial function is usually used in RSM [9]:

$$y = \beta_0 + \sum_{i=1}^{k} \beta_i x_i + \sum_{i=1}^{k} \beta_{ii} x_i^2 + \sum_{i} \sum_{j} \beta_{ij} x_i x_j + \varepsilon \tag{2}$$

where β_0 is a constant value, β_i are linear coefficients, β_{ii} are second order coefficients, β_{ij} are interaction coefficients and ε is the error of the regression equation.

2.2 Desirability approach

Many response surface problems involve the analysis of several responses. Simultaneous consideration of multiple responses involves first building an appropriate response surface model for each response and then trying to find

a set of operating condition that in some sense optimizes all responses or at least keeps them in desired ranges. The desirability method is recommended due to its simplicity, availability in the software and provides flexibility in weighting and giving importance for individual response. The desirability method is a simultaneous optimization technique which popularized by Drringer and Suich [21].

Solving such multiple response optimization problems employing this technique involves using a technique for combining multiple responses into a dimensionless measure of performance called the overall desirability function. The general approach is to first convert each response, Y_i, into a unitless utility bounded by $0<d_i<1$, where a higher d_i value indicates that response value Y_i is more desirable, and if the response is outside an acceptable region, $d_i=0$. Then, the design variables are chosen to maximize the overall desirability [4]:

$$D = \left(d_1.d_2....d_m\right)^{1/m} \tag{3}$$

where m is the number of responses. In the current work the individual desirability of each response was calculated using Equations (6) to (10).

The shape of the desirability function depends on the weight field, r. Weights are used to emphasize the target value. When the weight value is equal to 1, this will make the desirability function in linear mode. Choosing $r>1$ places more emphasis on being close to the target value, and choosing $0<r<1$ makes this less important [22]. If the target, T, for the response y is a maximum value, the desirability, d, will be defined by

$$d = \begin{cases} 0 & y < L \\ \left(\dfrac{y-L}{T-L}\right)^r & L \le y \le T \\ 1 & y > T \end{cases} \tag{4}$$

For the goal of minimum, the desirability will be defined by

$$d = \begin{cases} 1 & y < L \\ \left(\dfrac{T-y}{T-L}\right)^r & L \le y \le T \\ 0 & y > T \end{cases} \tag{5}$$

If the target is located between the lower, L, and upper, U, limits, the desirability will be defined by

$$d = \begin{cases} 0 & y < L \\ \left(\dfrac{y-L}{T-L}\right)^r & y < L \\ \left(\dfrac{T-y}{T-L}\right)^r & L \le y \le T \\ 0 & y > T \end{cases} \tag{6}$$

3 EXPERIMENTAL WORK

The material used in this research is Ni-based Rene 80 super alloy, whose chemical properties are shown in Table 1.

To improve the weldability of the Rene 80 workpiece, precipitated hardening heat treatment process is performed on the casted material [23]. In the previous research [10] using electrical discharge wire cutting, samples in 30 × 30 mm^2 dimensions and 1.4 mm thicknesses have been cut. To improve the contact between the two specimens and prevent passing through of the CO_2 laser beam, the specimens were finely ground on the welding side. This procedure removes the oxide layer caused by wire cutting and enhance the surface of the sample edge quality up to 0.8 μm.

Laser beam welding was performed by using a CO_2 laser (Optimal CO_2 laser machine; PRIMA Industries) emitting a multimode beam at 10.6 μm in the CW mode with a maximum power of 2200 W. Variation ranges of parameters were specified by performing several preliminary welding experiments, changing each parameter while other parameters were fixed. Full penetration, suitable appearance and immunity of defects were the parameters to discriminate the variables ranges. To improve the contact between the two specimens and prevent samples from experiencing any thermal twisting and the corresponding direction of the CO_2 laser beam with joint seam, a specially designed clamping device was used.

In order to study the weld geometrical dimensions, metallographic samples were etched in the Marbel's regent ($CuSO_4$ 4 gr, HCl 20 ml, water 20 ml). Weld surface width, W_1, weld pool area, A, width of the HAZ, W_2, under-

TABLE 1
Chemical composition of Ni-base superalloy Rene 80 (wt.%).

Ni	Cr	Co	Ti	W	Mo	Al	C	B	Fe	Zr
Bal	15.0	9.0	5.0	4.0	4.0	3.0	0.15	0.13	0.10	0.03

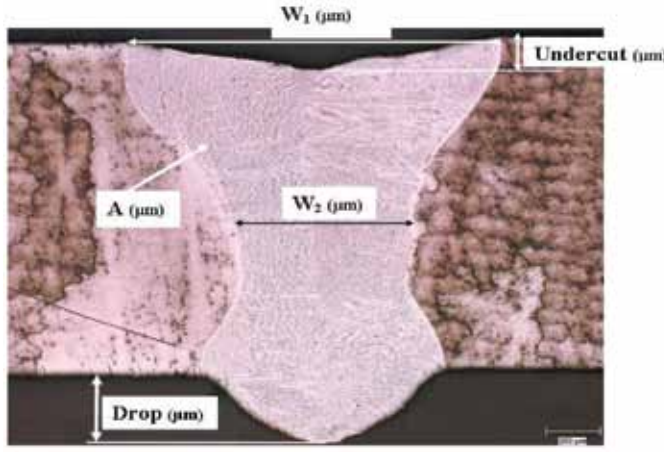

FIGURE 1
Optical micrograph showing the specimen cross-section and geometrical responses [9].

cut of welding and drop of welding process which are shown in Figure 1, were measured. Figure 1 indicates the cross-section of the weld pool and the location of geometrical responses.

4 OPTIMIZATION

After statistical analysis of the experimental data the regression's equations were derived to state the logical relationships between input and output parameters [8]:

$$W_1=1103.05+0.055P-206.19S+0.567F-12.042G+93.93S^2 +55.33P\times S+65.46P\times F+27.4P\times G-35.27S\times F-23.53S\times G-26.85F\times G \quad (7)$$

$$A=1028746+42043P-209308S+33571.8F+128471S^2 \quad (8)$$

$$W_2=546.17+19.03P-72.56S+14.33F-20.79G +61.16S^2-14.8G^2+24.5F\times G \quad (9)$$

$$U_c=20.612+81.921S-21.571G-33.21S^2 \quad (10)$$

and

TABLE 2
Constraints and criteria of input parameters and responses in this research.

		Parameter/Response	Goal	Lower	Target	Upper	Weight	Importance
Parameters		Laser power	Is in range	1	---	2.2	---	---
		Welding speed	Is in range	120	---	360	---	---
		Focal Plain position	Is in range	-0.5	---	0.5	---	---
		Inert gas pressure	Is in range	0.2	---	1	---	---
Response	Criteria 1	A	Minimize	870000	---	2000000	1	5
		W1	Minimize	742.38	---	1911	1	5
		W2	Minimize	428.1	---	989.44	1	3
		Undercut	Target	-268	0	108.2	1	3
		Drop	Target	36.15	37	319.4	1	3
	Criteria 2	A	Target	870000	900000	2000000	1	5
		W1	Target	742.38	750	1911	1	5
		W2	Target	428.1	450	989.44	1	3
		Undercut	Target	-268	0	108.2	1	3
		Drop	Target	36.15	37	319.4	1	3
	Criteria 3	A	Minimize	870000	---	2000000	1	5
		W1	Minimize	742.38	---	1911	1	5
		W2	Minimize	428.1	---	989.44	1	3
		Undercut	Minimize	-268	---	108.2	1	3
		Drop	Minimize	36.15	---	319.4	1	3

$$D_r=133.214-9.23P-55.55S+20.01F+31.22G +20.02S^2+16.44F^2-36.55P\times G \quad (11)$$

where P, S, F and G are laser power, welding speed, laser beam focal position and inert gas pressure, respectively. Physical inferences and presented diagrams in the previous research [10] certify the accuracy of the equations. Geometrical dimensions of the HAZ have a reverse relation with mechanical characteristics and joint strength. Accordingly, while complete weld penetration, one can achieve proper mechanical strength for joint by minimizing weld geometry dimensions.

In the present research, according to above discussion, the optimization of laser welding process was carried out in order to access optimum welding settings that result in minimal geometrical dimensions. Table 2 summarizes criterions in order to optimizing process parameters. In Table 2, W_1, A, and W_2 are welding surface width, weld pool area and width of the HAZ, respectively. In the optimization procedure presented in Table 2, the weight value of all three responses are the same (r=1).

According to Section 2.2, the optimization was performed according to criteria mentioned in Table 2 and utilizing response optimizer within DOE module of Minitab release 17. Optimum settings were obtained as presented in Table 3. The optimization results validate results of previous researches. After achieving full penetration welding, in the case of increasing laser power, one should increase the welding speed too. Focal position of laser beam and inert gas pressure are evaluated according to interaction with other parameters, in order to satisfy the welding condition.

5 RESULTS AND DISCUSSION

Experiments were carried out under optimum setups in order to validate the optimization results. Metallography of welded samples was performed as mentioned previously and the geometrical dimensions of HAZ were measured by Image Analysis software. Optimum conditions for laser welding, real and predicted weld geometrical dimensions and the errors are presented in table 3. Error percentage is regarded as the ratio of absolute value of difference toward real amount. As it is shown, the results validate high precision of optimization.

In the optimum configuration the tensile strength and microhardness of the as cast and heat treated weldments have been studied. So, the weld tensile strength test was performed in order to study mechanical characteristics of the joint in accordance with ASME sec. IX:2004 standard by using universal tensile test machine. Tensile test samples were prepared by electrical discharge wire cut machine. Table 4 indicates the results of welding tensile tests.

It is shown that Sample #2, with minimum geometrical dimensions according to Table 3, has the highest tensile strength and elongation. It can be inferred that by minimizing the geometrical dimensions of HAZ, the tensile strength will be maximized. Figure 2 shows the stress-strains diagram of the Sample #2 which is obtained from tensile strength test. It is considerable that welded samples were fractured from base metal in the optimum setup as shown in Figure 3; therefore, tensile strength of welded metal is greater than those of basic metal.

Also, the microhardness of weld pool for metallographic samples was measured based on ASTM E384 under a force 500 g. Figure 4 shows the microhardness measuring path in cross-section of the welding area. The microhardness distribution around the welding line is shown in Figure 5 for Sample #2. According to results, the hardness in weld pool is relatively more than base metal.

6 CONCLUSIONS

According to the performed optimization and CO_2 laser welding experiments, the metallographic tests and tensile strength tests, the following results can be concluded:

TABLE 3
Validation test result

Exp. No.	P(W)	S (cm/min)	F (mm)	G (bar)	D		W1	W2	A	Drop	Undercut
1	2200.000	249.00	-0.337	0.898	0.91042	Actual	1174	560.4	1140280.1	52.6	20.5
						Predicted	1225.9959	531.7986	1039000	47.3042	22.3126
						Error %	-4.428	5.103	8.882	10.068	-8.841
2	2190.052	255.045	-0.272	0.877	0.88756	Actual	1120	484.6	1121022.8	46.9	10
						Predicted	1085.4368	459.3079	1030000	43.5572	9.1425
						Error %	3.086	5.219	8.119	7.127	8.575
3	2200.000	240.00	-0.375	0.784	0.85151	Actual	1080	531	1215943.4	91.8	8.6
						Predicted	1040.448	497.2346	1062000	83.0819	7.7661
						Error %	3.662	6.358	12.660	9.496	9.696

TABLE 4
CO_2 laser welding tensile test results.

Exp. No.	Yield strength (N/mm2)	UTS (N/mm2)	Elongation (%)	Fracture Location
1	791.1	830.7	2.6	Base metal
2	810.8	886.0	5.3	Base metal
3	795.2	847.3	1.3	Base metal

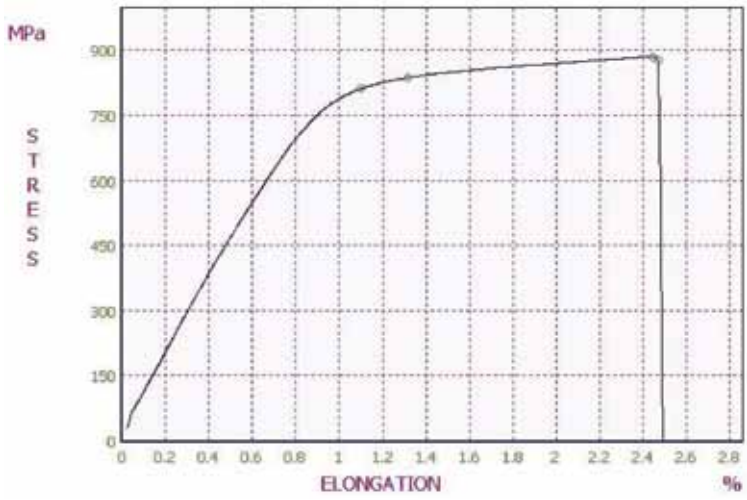

FIGURE 2
Stress-strains diagram for Sample #2.

FIGURE 3
Photograph of the fractured tensile specimen for Sample #2.

(i) Response surface methodology (RSM) methodology optimization results have a good agreement with experimental data, so this method could be suitable for modelling and optimization of laser welding processes;
(ii) Under condition of full penetration welding, geometrical dimensions of weld pool has got inverse effect on strength of the joint, so that by minimizing geometrical dimensions of weld pool, the tensile strength of welding will be increased;

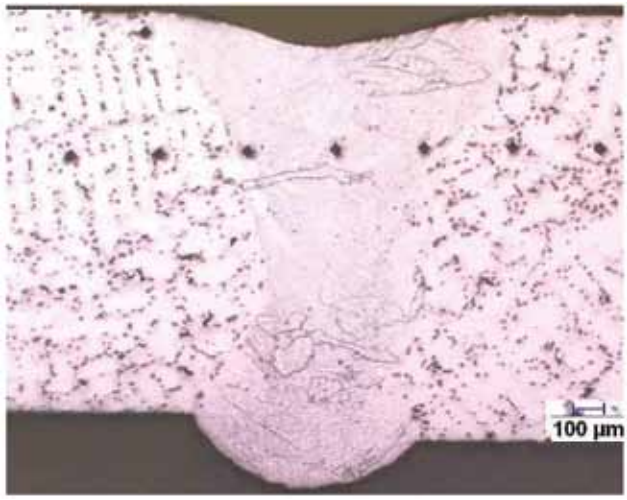

FIGURE 4
Optical micrograph with indentation marks across the weld zone of the Rene 80 weldments.

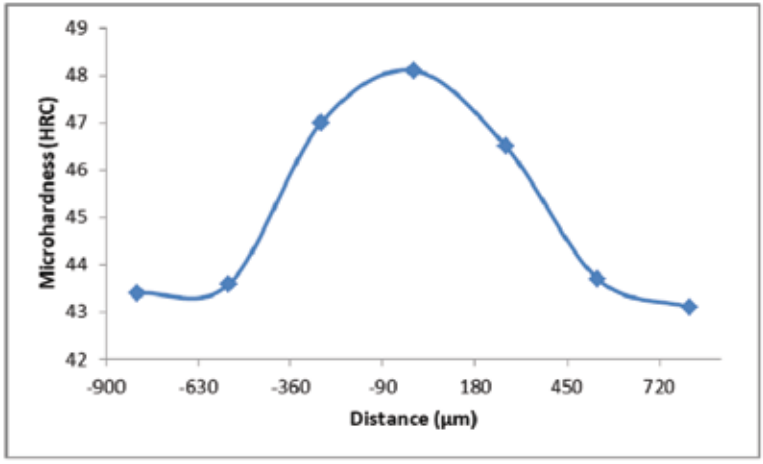

FIGURE 5
Microhardness profiles of the weld bead and parent metal.

(iii) By performing the optimization process the settings of: welding speed=255.045 cm/min; laser power=2190.052 W; focal position of the laser beam=-0.27213; and pressure of the inert gas=0.877434 bar can be regarded as the optimal settings of the CO_2 laser welding process in this research; and

(iv) Fracture location in tensile strength test of weldment in optimized setting is on base metal that reveals more strength of the weld zone metal towards the base metal in finally optimized setting.

NOMENCLATURE

A	Weld pool area (mm^2)
d	Desirability
D_r	Drop (μm)
F	Laser beam focal position (mm)
G	Inert gas pressure (bar)
k	Number of independent variables
L	Upper limit
m	Number of responses
P	Laser power (W)
r	Weight field
S	Welding speed (cm/min)
T	Target
U	Lower limit
U_c	Undercut (μm)
W_1	Welding surface width
W_2	Welding width of heat affected zone
X	Independent variable
Y	Response surface

Greek symbols

β_0	Constant
β_i	Linear coefficient
β_{ii}	Second order coefficient
β_{ij}	Interaction coefficient
ε	Error of the regression equation

REFERENCES

[1] Dawes C.T. *Laser Welding, a Practical Guide*. Cambridge: Woodhead Publishing. 1992.
[2] Steen W.M. *Laser Material Processing*. London: Springer. 1991.
[3] Duley W.W. *Laser Welding*. New York: Wiley-Intersience. 1998.
[4] Montgomery D.C. *Design and Analysis of Experiments.* New York: Wiley. 2005.
[5] Moradi M. and Mohazabpak A. Statistical modelling and optimization of laser percussion micro-drilling on Inconel 718 sheet using response surface methodology. *Lasers in Engineering* **39**(4-6) (2018), 313-331.

[6] Moradi M., Mehrabi O., Azdast T. and Benyounis K.Y. Enhancement of low power CO_2 laser cutting process for injection moulded polycarbonate. *Optics & Laser Technology* **96** (2017), 208–218.

[7] Moradi M. and Golchin E. Investigation on the effects of process parameters on laser percussion drilling using finite element methodology: Statistical modelling and optimization. *Latin American Journal of Solids and Structures* **14**(3) (2017), 464-484.

[8] Wang K.K. and Rasmussen G. Optimization of inertia welding process by response surface methodology. *Journal of Engineering for Industry* **94**(4) (1972), 999–1006.

[9] Benyounis K.Y., Olabi A.G. and Hashmi M.S.J. Multi-response optimization of CO_2 laser-welding process of austenitic stainless steel. *Optic & Laser Technology* **40** (2008), 76-87.

[10] Moradi M., Ghoreishi M. Investigation on laser welding parameters of weld-bead profile geometry of Ni-base superalloy Rene 80. *The International Journal of Advanced Manufacturing Technology* **55**(1-4) (2011), 205-215.

[11] Anawa E.M. and Olabi A.G. Optimization of tensile strength of ferritic/austenitic laser-welded Components. *Optics and Lasers in Engineering* **46** (2008), 571-577.

[12] Olabi A.G., Casalino G., Benyounis K.Y. and Rotondo A. Minimisation of the residual stress in the heat affected zone by means of numerical methods. *Materials & Design* **28** (2007), 2295-2302.

[13] Torabi A. and Kolahan F. Optimizing pulsed Nd:YAG laser beam welding process parameters to attain maximum ultimate tensile strength for thin AISI316L sheet using response surface methodology and simulated annealing algorithm. *Optics & Laser Technology* **103** (2018), 300–310.

[14] Kumara C., Dasa M., Paul C.P. and Singh B. Experimental investigation and metallographic characterization of fiber laser beam welding of Ti-6Al-4V alloy using response surface method. *Optics and Lasers in Engineering* **95** (2017), 52–68.

[15] Pakmanesh M.R. and Shamanian M. Optimization of pulsed laser welding process parameters in order to attain minimum underfill and undercut defects in thin 316L stainless steel foils. *Optics & Laser Technology* **99** (2018), 30–38.

[16] Khan M.M.A., Romoli L., Fiaschi M., Dini G. and Sarri F. Multiresponse optimization of laser welding of stainless steels in a constrained fillet joint configuration using RSM. *International Journal of Advanced Manufacturing Technology* **62** (2012), 587–603.

[17] Pakniat M., Ghaini F.M. and Torkamany M.J. Hot cracking in laser welding of Hastelloy X with pulsed Nd:YAG and continuous wave fiber lasers. *Materials & Design* **106** (2016), 177–183.

[18] Abdollahi H., Mahdavinejad R., Ghambari M. and Moradi M. Investigation of green properties of iron/jet-milled grey cast iron compacts by response surface method. *Proceedings of the Institution of Mechanical Engineers, Part B: Journal of Engineering Manufacture* **228**(4) (2014), 493-503.

[19] Azadi M., Azadi S., Zahedi F. and Moradi M. Multidisciplinary optimization of a car component under NVH and weight constraints using RSM. *International Mechanical Engineering Congress and Exposition (ASME 2009)*, 13–19 November **2009**, Lake Buena Vista, FL., USA. pp. 315-319.

[20] Shaikh Mohammad Meiabadi M.S., Kazerooni A. and Moradi M. Numerical analysis of laser assisted titanium to polyimide welding using statistical approach. *International Journal of Laser Science: Fundamental Theory and Analytical Methods* **1**(2) (2018), 185-205.

[21] Derringer G. and Suich R. Simultaneous optimization of several response variables. *Journal of Quality Technology* **12**(4) (1980), 214-219.

[22] Myers R.H., Montgomery D.C. and Anderson-Cook C.M. *Response Surface Methodology: Process and Product Optimization Using Designed Experiments*. New York: Wiley. 2009.

[23] Moradi M., Bakhish L. and Ghoreishi M. Investigating the effects of over aging heat treatment on Ni alloy Rene 80 microstructure. *The 10th Iranian Conference on Manufacturing Engineering (ICME 2010)*. 1-3 March 2010, Babol, Iran. pp. 223-231.